Enantiocomplementary continuous-flow synthesis of 2-aminobutane using covalently immobilized transaminases

Christian M. Heckmann,[†] Beatriz Dominguez,[‡] Francesca Paradisi[†,§*]

[†] School of Chemistry, University of Nottingham, University Park, Nottingham, NG7 2RD, UK

[‡] Johnson Matthey, 28 Cambridge Science Park, Milton Road, Cambridge, CB4 0FP, UK

[§] Dept. of Chemistry and Biochemistry, University of Bern, Freiestrasse 3, CH-3012, Bern, Switzerland.

*Corresponding author: francesca.paradisi@dcb.unibe.ch

Abstract

Chiral amines are a common feature of many active pharmaceutical ingredients. The synthesis of very small chiral amines is particularly challenging, even via biocatalytic routes, as the level of discrimination between similarly sized R-groups must be exceptional. Yet, their synthesis creates attractive building blocks that may then be used to prepare diverse compounds in further steps. Herein, the synthesis of one of the smallest chiral amines, 2-aminobutane, using transaminases, is being investigated. After screening a panel of mainly wild-type transaminases, two candidates were identified: an (*S*)-selective transaminase from *Halomonas elongata* (HEwT), and a pre-commercial (*R*)-selective transaminase from Johnson Matthey (*RTA-X43). Notably, a single strategic point mutation enhanced the enantioselectivity of HEwT from 45% *ee* to >99.5% *ee*. By covalently immobilizing these candidates, both enantiomers of 2-aminobutane were synthesized on a multi-gram scale, and the feasibility of isolation by distillation without the need for any solvents other than water was demonstrated. The atom economy of the process was calculated to be 56% and the E-factors (including waste generated during enzyme expression and immobilization) were 55 and 48 for the synthesis of (*R*)-2-aminobutane and (*S*)-2-aminobutane, respectively.

Keywords

Biocatalysis, amino transferase, chiral amine, enzyme engineering, process development

Introduction

Transaminases (TAs) have proven to be a valuable tool in the amine synthesis toolbox, with significant focus on producing chiral bulky amines in particular.[1] However, the use of TAs in the synthesis of smaller chiral amines is potentially advantageous as those building blocks may then be incorporated in subsequent syntheses generating additional diversity. One of the smallest chiral amines, 2-aminobutane, is a feature of the drug candidate XL888 (**Figure 1**), a HSP90 inhibitor currently in phase I clinical trials for use in conjunction with antibodies to treat cancer,[2–5] and it also appears in the herbicide Bromacil, which is commonly available as the racemate although the different enantiomers have been shown to have different effects.[6] In addition, 2-aminobutane is a feature of other clinically relevant molecules (for example in PET tracers[7] and featured in recent structure-activity relationship studies (SARs)[8,9]). In each case it is usually one enantiomer that is of interest. At the time of writing, the price for 1 g of (*S*)-2-aminobutane and (*R*)-2-aminobutane was 137 GBP and 136 GBP, respectively (Sigma Aldrich). In contrast, the price for 100 mL of racemic 2-aminobutane was 19.10 GBP (Sigma Aldrich).

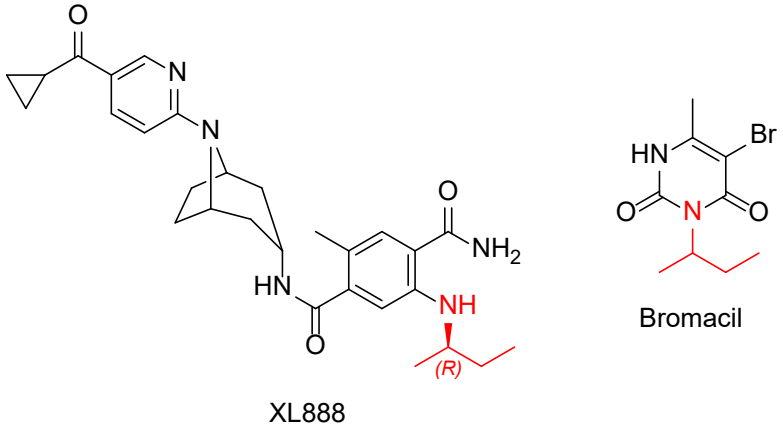

Figure 1: Structures of XL888 and Bromacil, the 2-aminobutane moiety is highlighted in red.

The similar size of the R-groups (ethyl vs methyl) poses a challenge in achieving high enantioselectivity. Racemic 2-aminobutane may be separated into its enantiomers by classical resolution using tartaric acid.[10] A recently reported asymmetric synthesis employing a chiral ruthenium catalyst only achieved 22% *ee*, among the lowest enantioselectivities for the substrates tried by the authors.[11] Kinetic resolution of 2-aminobutane using CAL-B, the dominant process used for making chiral amine building blocks (BASF process), requires ethyl decanoate as the acyl donor to achieve high enantioselectivity but is low yielding (25% yield, 99.8% *ee* (*S*) on a 5 g scale).[12] A dynamic kinetic resolution using the more conventional methyl 3-methoxypropionate resulted in 84% yield, 74% *ee* of the (*R*)-amide, on a 1 mmol

scale.[13] Kinetic resolutions employing several transaminases have also been investigated.[14–17] Deracemization via sequential addition of two enantiocomplementary transaminases was reported on a 50 mM scale by Kroutil and co-workers, giving either enantiomer (>99% conversion, >99% *ee*) depending on the order of addition of the transaminases.[18]

Syntheses of 2-aminobutane from butanone with transaminases have also been reported,[19–21] using alanine as the donor with a coupled enzymatic pyruvate removal, achieving moderate to excellent conversions (31–98%) and high enantioselectivities (>98% *ee*). However, intensification beyond 50 mM and the use of the simpler isopropylamine (IPA) as the amine donor have not been investigated. In addition, isolation of the 2-aminobutane product has not been attempted, presumably due to its high solubility in water and high volatility. Herein, we report the synthesis of both enantiomers of 2-aminobutane with excellent enantioselectivity and good conversions on a 300 mM scale, using immobilized transaminases in flow, as well as the isolation of 2-aminobutane by distillation from the reaction mixture. In addition, we present how the creation of a rationally designed mutant variant of an (*S*)-selective transaminase, dramatically increased the optical purity of the product.

Materials and Methods

Flow biocatalysis was carried out using an R-series modular flow chemistry system from Vapourtec. Relizyme resins for protein immobilization were kindly donated by Residion. Reagents and cofactors were purchased from Sigma Aldrich, Thermo Fisher, Apollo Scientific, or Alfa Aesar and used without further purification. Enzymes were prepared in-house (see electronic supporting information) or provided by Johnson Matthey (RTA-40; RTA-57; *RTA-43; RTA-25; STA-1; STA-2 STA-13; STA-14, where the * indicates a pre-commercial enzyme and the numbers refer to the product code). NMR spectra were obtained using a Bruker 400 MHz NMR spectrometer (Bruker AV3400 or AV3400HD) and referenced relative to the residual protonated solvent peak. ESI-MS data were obtained on a Bruker MicroTOF spectrometer.

Batch Biotransformations—IPA method

Reactions were set up containing butanone (10-300 mM) and IPA (5 eq.), lyophilized TA cfe (50 mg/mmol), and PLP (1 mM) in potassium phosphate buffer (50 mM pH 8), in a final volume of 500 µL to 1 mL. Reactions were incubated at 30 °C, with gentle shaking in duplicate. Samples were removed, diluted appropriately (total amine content <25 mM), FMOC-derivatized and analysed by LC-MS or reverse-phase HPLC. Enantiopreference was determined by chiral GC-FID or chiral reverse-phase HPLC.

Enzyme immobilization

Based on the technique previously applied to the STA HEwT,[22,23] resin (Relizyme EP403/S or epoxy-agarose[24]) was incubated in modification buffer (2 mL/g_{resin}; 100 mM sodium borate, saturated (approx. 2 M) iminodiacetic acid, pH 8.5) at ambient temperature with gentle shaking for 2 h. The resin was removed by vacuum filtration, washed with dH_2O, and incubated in metal buffer (5 mL/g_{resin}; 1 M sodium chloride, 5 mg/mL cobalt(II) chloride hexahydrate) at ambient temperature with gentle shaking for 2h. Following filtration and washing, the resin was suspended in storage buffer (potassium phosphate 50 mM, pH 8, 0.1 mM PLP) containing the enzyme (varying concentrations and ratios with respect to resin, to achieve the desired loading) and gently shaken at ambient temperature. The incubation time was determined from test immobilizations and the remaining protein concentration and activity in the supernatant, typically 3-5 h. The resin was filtered and washed, suspended in desorption buffer (4 mL/g_{resin}; 50 mM EDTA, 500 mM sodium chloride, 20 mM potassium phosphate, pH 7.4), filtered and washed again, and suspended in blocking buffer (4 mL/g_{resin}; saturated (approx. 3 M) glycine, 0.1 mM PLP, pH 8.5). Following incubation at ambient temperature with gentle shaking for 20 h the resin was filtered off, washed, and stored in storage buffer at 4 °C. Samples of each washing step were taken and analysed by SDS-PAGE. Resin with immobilized *Ts*RTA was boiled in SDS-loading buffer. The activity of the resin was determined by shaking an appropriate amount of resin in standard assay buffer, taking samples periodically and measuring the increase in UV absorbance at 245 nm (samples were re-added after measurement).

Scaled-up 2-aminobutane synthesis in flow

Two Omnifit glass columns (6.6 mm i.d. × 150 mm length) were employed in series, giving a combined packed-bed volume of 7.73 mL (using 6 g_{resin}) (see **Figure S1** for a photo and scheme of the reactor set-up). The reactor was equilibrated with storage buffer (potassium phosphate 50 mM, pH 8, 0.1 mM PLP) for 5 CV at a flowrate of 0.5 mL/min. For reactor start-up, the reaction mixture (butanone (300 mM), IPA (1.5 M) and PLP (1 mM) in potassium phosphate buffer (50 mM, pH 8)) was passed through the reactor at a flow-rate of 0.5 mL/min at ambient temperature until it reached the outlet. At this point, the output was fed back into the vessel containing the reaction mixture and the reaction was run in circulation mode using a residence time of 25 min per pass (0.309 ml/min), at 30 °C. The reaction mixture was circulated until 4 h of contact time between the reaction mixture and resin (corresponding to 9.6 passes) was reached, at which point the inlet was moved to a fresh reaction mixture. After the volume remaining in the reactor and tubing was collected, the outlet was also moved to the fresh reaction mixture

which was then circulated as before. The swapping of the reaction mixture was carried out every 1-4 days (corresponding to 6-24 CV) and the reactor was left running for 165 h in total (1 week). For reactor shutdown, the inlet was placed in storage buffer and the remaining reaction mixture was flushed out of the tubing at a flowrate of 0.5 mL/min at ambient temperature. All processed reaction mixtures were combined, acidified using hydrochloric acid (pH <1) and concentrated (to approximately 60% of the initial weight) *in-vacuo*, removing the ketones. The remaining aqueous solution was alkalized with an excess of potassium hydroxide (approx. 33 g) and distilled under atmospheric pressure. Three cuts (b.p. ≤38 °C, 38–50 °C, and 46–65 °C) were obtained that contained both IPA and 2-aminobutane, with the proportion of the latter increasing in the higher b.p. cuts (as determined by ^{1}H-NMR, **Table S1**). These cuts were then redistilled over potassium hydroxide employing a fractional distillation set-up using a four-ball Snyder column, obtaining four cuts (b.p. ≤32 °C, 32–34°C, 34–62 °C, and 62 °C). Cuts one and two were virtually pure IPA, cut three was a mixture of IPA and 2-aminobutane, and cut four was 2-aminobutane with ≤1% IPA as determined by ^{1}H-NMR (**Table S1**), giving 2.49 g of (*S*)-2-aminobutane (35% yield, ≥99% purity (^{1}H-NMR), >99.5% *ee*) and 1.97 g of (*R*)-2-aminobutane (28% yield, ≥99% purity (^{1}H-NMR), 98.7% *ee*), from the HEwT_F84W and *RTA-43 flow reactions, respectively.

(*S*)-2-aminobutane: ^{1}H-NMR (400 MHz, $CDCl_3$) δ 2.79 (1 H, h, *J* 6.3, C*H*N), 1.37–1.26 (2 H, m, CH_2), 1.15 (2 H, br s, NH_2), 1.02 (3 H, d, *J* 6.3, CHNCH_3), 0.87 (3 H, t, *J* 7.4, CH_2CH_3); ^{13}C-NMR (101 MHz, $CDCl_3$) δ 48.4 (*C*HN), 32.9 (CH_2), 23.4 ($CHNCH_3$), 10.6 (CH_2CH_3); in agreement with lit.[25] *m/z* $[M+H]^+$ calculated: 74.0964, found: 74.0956.

(*R*)-2-aminobutane: ^{1}H-NMR (400 MHz, $CDCl_3$) δ 2.77 (1 H, h, *J* 6.3, C*H*N), 1.38–1.26 (2 H, m, CH_2), 1.18 (2 H, br s, NH_2), 1.03 (3 H, d, *J* 6.3, CHNCH_3), 0.88 (3 H, t, *J* 7.4, CH_2CH_3); ^{13}C-NMR (101 MHz, $CDCl_3$) δ 48.4 (*C*HN), 32.8 (CH_2), 23.4 ($CHNCH_3$), 10.6 (CH_2CH_3); in agreement with lit.[25] *m/z* $[M+H]^+$ calculated: 74.0964, found: 74.0958.

Results and Discussion

Screening of STAs and RTAs against butanone

Initial screening was performed with 12 transaminases. In addition to the 8 transaminases from Johnson Matthey's portfolio, the STAs from *Halomonas elongata* (HEwT)[26] and *Chromobacterium violaceum* (*Cv*STA),[27] and the RTAs from *Thermomyces stellatus* (*Ts*RTA)[28] and *Aspergillus terreus* (*At*RTA)[29] were also screened. All enzymes were used as lyophilized cell-free extracts (cfes) and tested at three

substrate concentrations (10, 100 and 300 mM), using 5 equivalents of IPA while keeping a constant loading of enzyme relative to substrate of 50 mg/mmol (0.5-15 mg/mL) (**Scheme 1**). By fixing the enzyme loading in this way, the turnover number (TON) required to reach a certain conversion does not increase with increasing concentration. In addition to TON, different concentrations of active enzyme in the crude enzyme mix (see **Figure S2**) will also affect the conversion. While not correcting for active enzyme content may give a less precise indication of the specific performance of the catalyst, this was a deliberate choice as the crude lyophilizate is sold commercially by weight.

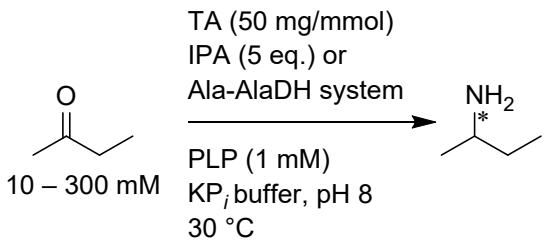

Scheme 1: Screening conditions for the transaminase catalysed synthesis of 2-aminobutane, starting from butanone. Ala-AlaDH system: L-Ala (1.2 eq.) or DL-Ala (2.4 eq.), AlaDH (25 mg/mmol), GDH (25 mg/mmol), D-glucose (1.2 eq.), NH_4Cl (2.4 eq.), and NAD^+ (1 mM). Ala-AlaDH: KP_i (300 mM), IPA: KP_i (50 mM) Enzymes were employed as lyophilized cfes.

Almost all enzymes screened exhibited an increase in conversions at the 5 h mark when going from 10 mM to 100 mM concentration (**Figure 2**). This is likely due to the enzymes not having high affinity for butanone. For some enzymes, such as STA-1 and -2, the conversions at 5 h decreased when scaling up to 300 mM, for others, such as *RTA-43, *Cv*STA, and, most notably, HEwT conversions further increased at the highest substrate concentration. While lower 5 h conversions at the highest substrate loading always corresponded to lower final conversions, the contrary was not always true for the enzymes performing better at the 5 h mark (as is the case for STA-14 and RTA-25).

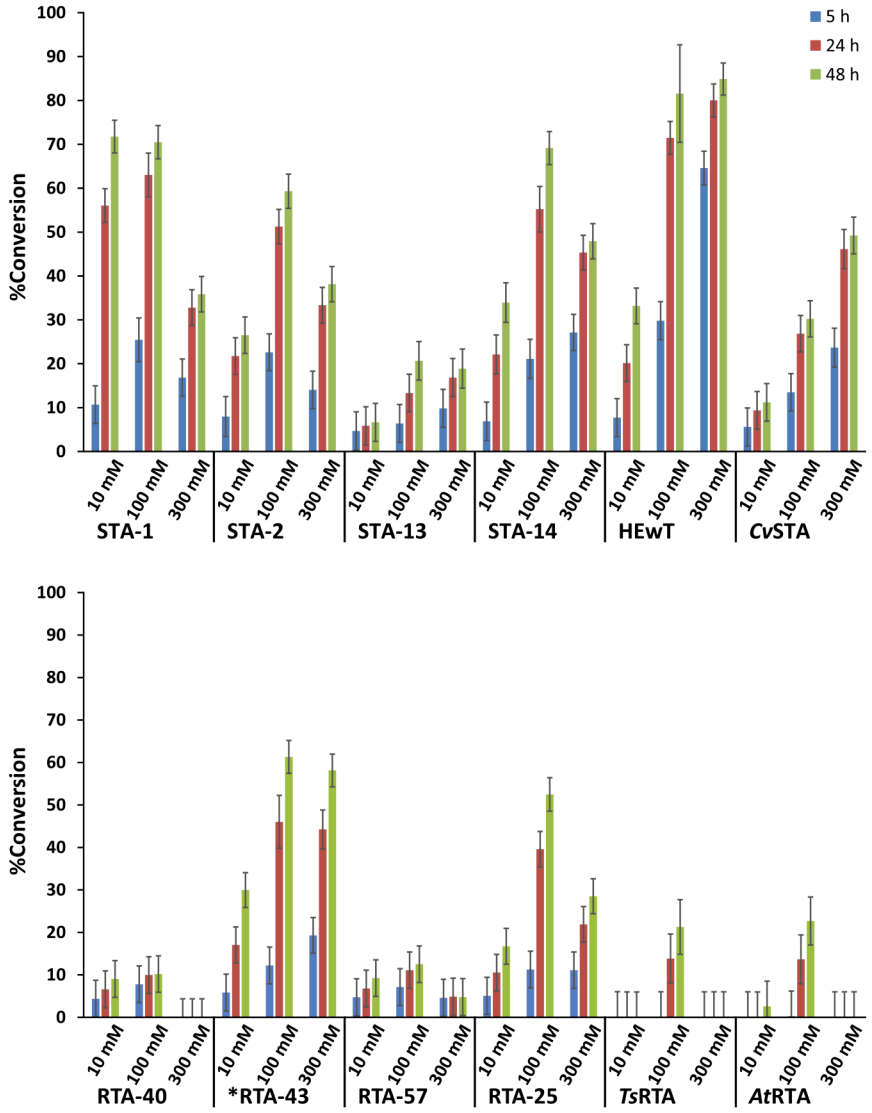

Figure 2: Transaminase screen: biotransformations of butanone, using IPA as the amine donor. Samples were taken after 5 h, 24 h, and 48 h, and conversions were determined following the production of 2-aminobutane by RP-HPLC, after FMOC derivatization, using a calibration curve. All experiments were carried out in duplicate, error bars represent the standard error (SE), and include the uncertainty associated with the calibration curve.[30,31]

Of the STAs tested, HEwT clearly outperformed the others in terms of conversions, reaching almost 70% at the 300 mM scale in 5 h, and achieving the highest final conversions (almost 90%). However, in terms of enantioselectivity it did poorly, yielding only 45% *ee* (*S*) (**Table 1**). *Cv*STA, which also showed a significant albeit smaller increase in conversion from 100 mM to 300 mM, also had an unsatisfactory 80% *ee*. For the RTAs, only *RTA-43 and -25 showed acceptable levels of conversion, with *RTA-43 giving better scalability. For all RTAs, the enantioselectivities were excellent.

Table 1: Enantiomeric excess (*ee*) of the biotransformations employing IPA as the amine donor.

	10 mM	100 mM	300 mM
STA-1	96% (*S*)	96% (*S*)	99% (*S*)
STA-2	traces (*S*)	99.5% (*S*)	99.6% (*S*)
STA-13	traces (*S*)	85% (*S*)	84% (*S*)
STA-14	97% (*S*)	94% (*S*)	96% (*S*)
HEwT	68% (*S*)	45% (*S*)	46% (*S*)
***Cv*STA**	traces (*S*)	79% (*S*)	81% (*S*)
RTA-40	traces (*R*)	traces (*R*)	traces (*R*)
***RTA-43**	>99% (*R*)[a]	99.4% (*R*)	99.4% (*R*)
RTA-57	traces (*R*)	>99% (*R*)[a]	traces (*R*)
RTA-25	traces (*R*)	99.3% (*R*)	99.6% (*R*)
***Ts*RTA**	>99.5% (*R*)[ab]	>99.5% (*R*)[ab]	n/d[b]
***At*RTA**	>99.5% (*R*)[ab]	>99.5% (*R*)[ab]	n/d[b]

All *ee*s represent the average of duplicates.
[a] other enantiomer not detected
[b] chiral RP-HPLC
n/d not detected

To evaluate whether the poorly performing enzymes were due to lack of acceptance of IPA, the screening was repeated with alanine as the amine donor, employing an AlaDH from Johnson Matthey and a glucose dehydrogenase (GDH) from *Bacillus megaterium*[32] for pyruvate recycling/removal. For the STAs, 1.2 equivalents of L-Ala were used as the donor, for the RTAs 2.4 equivalents of racemic alanine were used (effectively using 1.2 equivalents of D-Ala, **Scheme 1**). While all three enzymes showed improved performance using the new amine donor, in particular STA-13 and RTA-57 (**Figure S3**), they fell short of the best performing enzymes employing IPA. STA-13 gave a poor *ee* of 85% (**Table S2**), but an increase in conversion from 100 mM to 300 mM as had been observed for *Cv*STA and HEwT.

All RTAs were outperformed by *RTA-43 in terms of conversion (all RTAs had excellent *ee*, **Table 1**) and this catalyst was chosen for the production of (*R*)-2-aminobutane. As its conversion still was lower than that observed for some of the STAs, the use of the Ala-AlaDH system to displace the pyruvate by-product was investigated, but this did not improve conversions (**Figure S3**). Among the STAs, STA-2 showed the highest *ee* of (*S*)-2-aminobutane; yet had slightly lower conversions compared to STA-1 and STA-14, both of which still had >90% *ee*. More importantly, all three enzymes showed a significant drop in conversion going from 100 mM to 300 mM. Engineering of HEwT to increase its enantioselectivity while retaining the excellent performance was therefore attempted.

To this end, two phenylalanine residues in the small pocket (**Figure 3**; F18 and F84) were independently changed to the larger tryptophan (chosen to maintain the aromaticity, as the F18 position in particular is highly conserved and sensitive to changes[33]). The residue F84 has been show previously to be a hot-spot for enlarging the small pocked in other STAs,[34,35] whereas no previous attempt to engineer an STA to enhance enantioselectivity for small substrates has been reported.

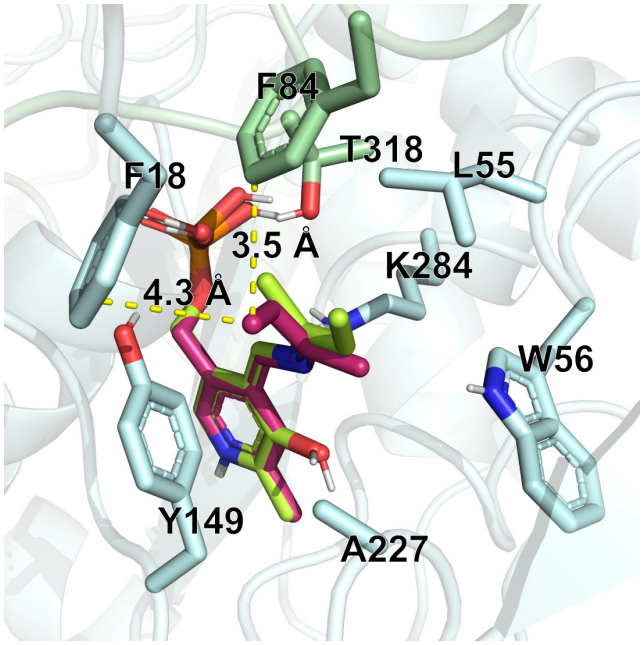

Figure 3: Docked quinonoid intermediate in the pro-(*S*) (lime) and pro-(*R*) (pink) orientation into the active site of HEwT (PDB: 6GWI).[36] Side-chains of residues surrounding the butane-amine moiety are shown as sticks; the two different subunits are coloured cyan and green. Distances of the ethyl-group in the pro-(*R*) orientation to F18 and F84 are shown. Docking was carried out using Autodock/vina,[37] the figure was generated using open source PyMOL 2.1.0.

While HEwT_F18W exhibited significantly lower conversions (in particular at 300 mM) and unchanged enantioselectivity (50-55% *ee* (*S*), see **Figure S20**), HEwT_F84W exclusively produced (*S*)-2-aminobutane (*ee* >99.5%) at all substrate concentrations. However, reaction rate and final conversion were reduced compared to wild-type HEwT, in particular at 10 mM and 100 mM, but remained higher than for the other STAs at 300 mM (this is clear when comparing **Figure 2** and **Figure 4**). HEwT_F84W shows also a steady increase in conversion from 10 mM all the way through to 300 mM. This suggests that the increased steric bulk in the small pocket may reduce the affinity for butanone, which would also explain the slightly lower final conversions at 300 mM. However, attempts at measuring the K_m or the specific activity using the acetophenone assay[38] were unsuccessful, as the activity was too low to be measured (no activity was detected at up to 1mg/mL of enzyme and using 10-350 mM of butanone). The

specific activities with SMBA and pyruvate were 0.01 U/mg and 0.2 U/mg for the lyophilized crude HEwT_F84W and wild-type, respectively.

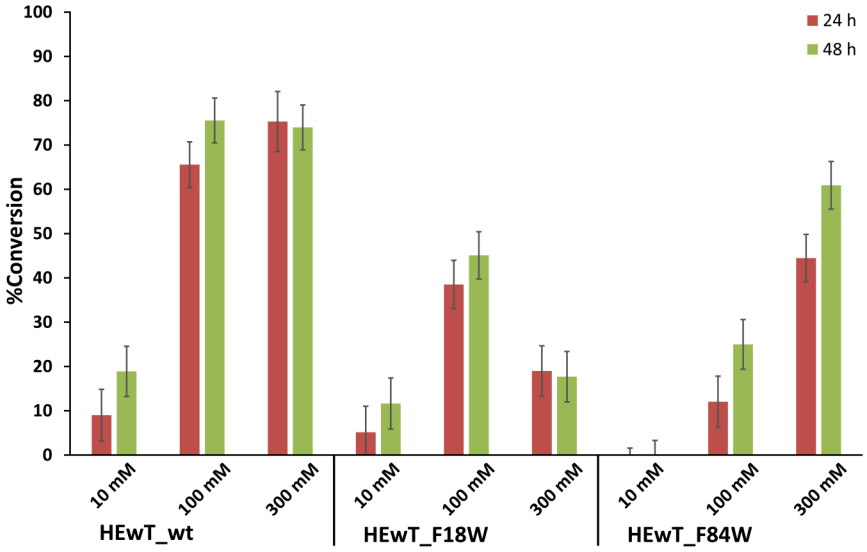

Figure 4: HEwT mutants: biotransformations of butanone, using IPA as the amine donor. Samples were taken after 24 h and 48 h, and conversions were determined following the production of 2-aminobutane by RP-HPLC, after FMOC derivatization, using a calibration curve. All experiments were carried out in duplicate, error bars represent the standard error (SE), and include the uncertainty associated with the calibration curve.[30,31]

Determination of immobilization and operating conditions in flow

As the batch reactions required high enzyme loading (15 mg/mL at the 300 mM concentration), enzyme immobilization and use in continuous flow, in a packed-bed reactor, were investigated, to facilitate reusability of the enzyme. Additionally, moving to flow has previously been shown to result in increased performance.[22] Initial immobilizations were carried out on Co^{II}-derivatized Relizyme EP403/S beads, using an initial loading of 100 mg_{lyo}/g_{resin}. For both *RTA-43 and HEwT_F84W, complete immobilization was achieved within 3-4 h, giving recovered activities of 50% and 30%, respectively, where the recovered activity is defined as the fraction of activity contained in the resin compared to the total activity offered to the resin. Using these resins, operating conditions in flow were explored. Given the long reaction times despite the high enzyme loading employed in batch, a reaction in a single pass proved unfeasible with the equipment available. Thus, a recirculating strategy was adopted, where the output was fed back into the reaction mixture. Increasing the reaction temperature to 37 °C resulted in a loss of activity of the immobilized enzyme, whereas both enzymes were able to operate for >24 h without any detectable loss in activity at 30 °C. Conversions after recirculating four column volumes of reaction mixture for 24 h (6 h contact time; approx. 9×40 min residence time) were 50% and 30% for *RTA-43 and

HEwT_F84W, respectively. Addition of DMSO or increasing the concentration of IPA did not improve performance.

Thus, the loading of enzyme on the resin was increased. Loadings of 170 mg_{lyo}/g_{resin} and 400 mg_{lyo}/g_{resin} were achieved for *RTA-43 and HEwT_F84W, respectively. At these loadings between 70-100% of the enzyme was immobilized (as determined from the residual activity of the supernatant). Further increasing the loading did not increase the amount of enzyme immobilized. Recovered activities reached up to 38% for *RTA-43 and up to 64% for HEwT_F84W. With these resins, conversions up to 75% were achieved in 4 h (approx. 12×20 min residence time), with no further increase with longer contact times.

Scale-up synthesis of both enantiomers of 2-aminobutane in flow

Using these operating conditions, larger scale syntheses of both enantiomers of 2-aminobutane were carried out. By employing 6 g of resin, 46.4 mL of reaction mixture could be processed every 24h. For each of the enzymes, the reactor was left running continuously for one week, replacing the reaction mixture every 1-4 days, processing a total volume of 0.319 L, containing 6.90 g (95.7 mmol) of butanone. Conversions were determined each time the reaction mixture was changed (**Figure 5**). For HEwT_F84W, conversions were stable over the duration of seven days (66±5%), and no loss in activity was detected in the resin afterwards. On the other hand, for *RTA-43 conversions dropped from 69±5% to 54±5% after seven days, and the specific activity of the resin decreased by 35%. Compared to the initial batch process, both catalyst productivity and Space-time yield have been improved, as envisaged (**Table 2**).

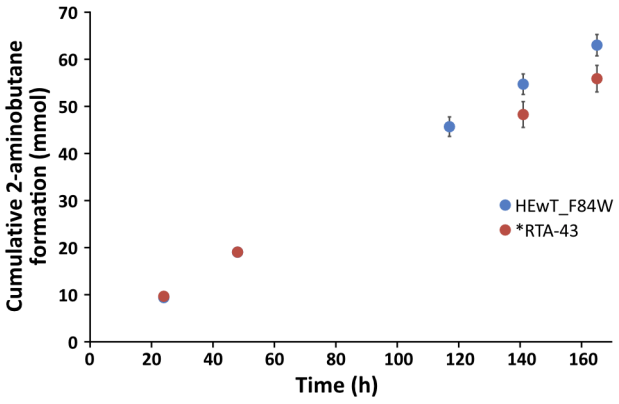

Figure 5: Cumulative production of 2-aminobutane during a 7-day run of the continuous flow process, employing either HEwT_F84W or *RTA-43. At each time point, the solution was replaced with a fresh reaction mixture and the conversion determined using RP-HPLC. Error bars represent standard error of the calibration curve. Data gaps between 48 h and 120 h or 144 h for HEwT_F84 and *RTA-43, respectively, are due to periods of lab-closure, where a proportionally larger volume of liquid was circulated.

Table 2: Comparison of key process parameters between the batch and flow process.

		Specific reaction rate (µmol mg^{-1} h^{-1})[a]	Catalyst productivity (µmol mg^{-1})[b]	Space-time yield (µmol mL^{-1} h^{-1})[c]
Batch	HEwT_F84W	0.293	14.1	4.40
	*RTA-43	0.267	12.8	4.00
Flow	HEwT_F84W	0.159	26.3	49.4
	*RTA-43	0.332	54.8	43.8

[a] Calculated according to $^{n_{BA}}/_{m_{lyo-cfe} \times t_{total}}$, at similar levels of conversions (achieved after 48 h in the case of batch reactions (**Figure 2**)), where n_{BA} corresponds to the overall amount of 2-aminobutane produced (as determined by HPLC), $m_{lyo-cfe}$ corresponds to the mass of lyophilized cfe used, and t_{total} corresponds to the total reaction time (48 h batch, 165 h flow). For the flow process, this has been calculated with respect to the amount of enzyme offered during the immobilization, neglecting any losses in activity.

[b] Calculated according to $^{n_{BA}}/_{m_{lyo-cfe}}$.

[c] Calculated as follows: batch: $^{n_{BA}}/_{V_{rxn} \times t_{total}}$, where V_{rxn} corresponds to the reaction volume. Flow: $^{n_{BA}}/_{V_{bed} \times t_{total}}$, where V_{bed} corresponds to the reactor bed volume.

Given the highly volatile and highly water-soluble nature of 2-aminobutane, as well as the similar structure to IPA, purification by distillation appeared to be the best approach, avoiding both the need for water removal as well as use of organic solvents. Alternative strategies, such as lyophilization for water removal or precipitation were also investigated (data not shown). However, preliminary tests had shown that when lyophilizing acidic solutions of 2-aminobutane and IPA in water, up to 25% of the initially added mass were lost, presumably due to the same apparent sublimation that is also observed for ammonium chloride. Precipitation of 2-aminobutane from the reaction mixture using tartaric acid[10] also proved to be ineffective (data not shown).

In a first vacuum distillation, the ketones were removed from an acidified reaction mixture. Subsequently, the remaining aqueous solution was alkalized, and the amines were distilled. However, separation of the amines during this initial distillation proved very challenging. Thus, a third fractional distillation (4-ball Snyder column) had to be employed on the amine mixture obtained from the second distillation, giving 2.49 g of (*S*)-2-aminobutane and 1.97 g of (*R*)-2-aminobutane, corresponding to a yield of 35% and 28%, respectively (*ee*s ≥99%). This represents a mass-loss of approx. 50%. While some of the apparently lost amine was contained in an impure cut (5% and 15% for (*S*)- and (*R*)-2-aminobutane, respectively), there was also loss through leaking joints and potentially during the initial vacuum distillation. However, this mass-loss should be reduced at a larger scale with a more effective (industrial)

distillation set-up. Additionally, combining the second distillation and fractional distillation might further reduce this mass-loss.

The use of alternative amino donors, cadaverine and alanine, was also explored in flow. Employing 4 eq. of cadaverine at pH 9 under otherwise identical conditions, HEwT_F84W lost 60% and *RTA-43 lost 75% of activity over 24 h. Additionally, conversions for *RTA-43 were reduced to 25% (employing cadaverine in batch using 2 or 4 eq. at pH 8 or 9 resulted in no conversion with *RTA-43). The conversion obtained with HEwT_F84W was unchanged at 68%. The use of alanine in flow was hampered by the lack of compatible supports for the covalent immobilization of the transaminases, GDH, and AlaDH (or LDH), as attempts to immobilize the GDH on EP403/S resulted in low recovered activities (data now shown). On the other hand, the transaminases were not operationally stable when immobilized on epoxy-agarose, the preferred support for GDH (data now shown).[32]

To assess the sustainability of this process, the atom economy and E-factor were calculated. The atom economy, defined as the molecular weight of the desired product divided by the molecular weight of all products, was 56%. The E-factor, which is defined as the mass of all waste (neglecting water) divided by the mass of product, was calculated with respect to the actual isolated yield obtained in this current work. The mass of the culture media and buffer salts used throughout, despite their benign nature (bio-renewable and bio-degradable in the case of culture media) has been taken into account. Additionally, the supported enzyme catalyst used in the flow reaction is considered waste, despite being potentially usable for further cycles (in particular in the case of HEwT_F84W). Furthermore, the recovered IPA may be re-used and the unreacted butanone could in principle be separated from the waste acetone, but this has also been ignored in the calculation. Thus, this E-factor represents a “worst-case” estimate (see Supporting information for detailed breakdown); and has been calculated to be 48 for the HEwT_F84W process and 55 for the *RTA-43 process.

Conclusions

Following the screening of a panel of transaminases, two enantiocomplementary transaminases for the synthesis of 2-aminobutane from butanone were identified. Employing a single strategic point mutation in the small binding pocket, the enantioselectivity of the STA showing the best conversion was enhanced from 45% *ee* to >99.5%, with only slight reduction in the conversions. By immobilizing the enzymes and moving to continuous flow reaction set up with the catalyst housed in a packed bed reactor, both enzymes could be used continuously for one week, producing either enantiomer of 2-aminobutane

at a multi-gram scale, while improving catalyst productivity and space-time yield relative to the batch process using soluble enzyme (**Table 2**). The isolation of 2-aminobutane from the reaction mixture using a simple distillation set-up was also demonstrated; however, further work to reduce losses in this step is however required to enhance the efficiency of the reaction. The atom economy of the process has been calculated to be 56%, and the E-factor was 48 and 55 for the STA and RTA process, respectively. Recycling of un-spend reagents, which are recovered from the mixture during the distillation (**Table S1**), as well as reducing losses during the purification will further improve the sustainability of this process.

Acknowledgements

This work was supported by the Biotechnology and Biological Sciences Research Council through the iCASE scheme in collaboration with Johnson Matthey [grant number BB/M008770/1].

Associated content

Supporting information. Additional detailed methods (Site-directed mutagenesis, Expression, Activity Assays, Batch biotransformations, Analytics), supporting figures, supporting tables, chromatograms for *ee*, and NMR spectra.

References

(1) Savile, C. K.; Janey, J. M.; Mundorff, E. C.; Moore, J. C.; Tam, S.; Jarvis, W. R.; Colbeck, J. C.; Krebber, A.; Fleitz, F. J.; Brands, J.; et al. Biocatalytic Asymmetric Synthesis of Chiral Amines from Ketones Applied to Sitagliptin Manufacture. *Science* **2010**, *329* (5989), 305–310. https://doi.org/10.1126/science.1188934.

(2) Azimi, A.; Caramuta, S.; Seashore-Ludlow, B.; Boström, J.; Robinson, J. L.; Edfors, F.; Tuominen, R.; Kemper, K.; Krijgsman, O.; Peeper, D. S.; et al. Targeting CDK2 Overcomes Melanoma Resistance against BRAF and Hsp90 Inhibitors. *Mol. Syst. Biol.* **2018**, *14* (3), e7858. https://doi.org/10.15252/msb.20177858.

(3) Pembrolizumab and Hsp90 inhibitor XL888 in Treating Patients with Advanced Gastrointestinal Cancer https://www.cancer.gov/about-cancer/treatment/clinical-trials/search/v?id=NCI-2016-01594&r=1 (accessed Mar 31, 2020).

(4) XL888 + Vemurafenib + Cobimetinib for Unresectable BRAF Mutated Stage III/IV Melanoma https://clinicaltrials.gov/ct2/show/NCT02721459 (accessed Mar 31, 2020).

(5) Study of XL888 With Vemurafenib for Patients With Unresectable BRAF Mutated Stage III/IV Melanoma https://clinicaltrials.gov/ct2/show/NCT01657591 (accessed Mar 31, 2020).

(6) Chen, Z.; Zou, Y.; Wang, J.; Li, M.; Wen, Y. Phytotoxicity of Chiral Herbicide Bromacil: Enantioselectivity of Photosynthesis in Arabidopsis Thaliana. *Sci. Total Environ.* **2016**, *548–549*, 139–147. https://doi.org/10.1016/j.scitotenv.2016.01.046.

(7) Berroterán-Infante, N.; Kalina, T.; Fetty, L.; Janisch, V.; Velasco, R.; Vraka, C.; Hacker, M.; Haug, A. R.;

Pallitsch, K.; Wadsak, W.; et al. (R)-[18F]NEBIFQUINIDE: A Promising New PET Tracer for TSPO Imaging. *Eur. J. Med. Chem.* **2019**, *176*, 410–418. https://doi.org/10.1016/j.ejmech.2019.05.008.

(8) Vandyck, K.; Rombouts, G.; Stoops, B.; Tahri, A.; Vos, A.; Verschueren, W.; Wu, Y.; Yang, J.; Hou, F.; Huang, B.; et al. Synthesis and Evaluation of N-Phenyl-3-Sulfamoyl-Benzamide Derivatives as Capsid Assembly Modulators Inhibiting Hepatitis B Virus (HBV). *J. Med. Chem.* **2018**, *61* (14), 6247–6260. https://doi.org/10.1021/acs.jmedchem.8b00654.

(9) Osborne, J.; Birchall, K.; Tsagris, D. J.; Lewis, S. J.; Smiljanic-Hurley, E.; Taylor, D. L.; Levy, A.; Alessi, D. R.; McIver, E. G. Discovery of Potent and Selective 5-Azaindazole Inhibitors of Leucine-Rich Repeat Kinase 2 (LRRK2) – Part 1. *Bioorg. Med. Chem. Lett.* **2019**, *29* (4), 668–673. https://doi.org/10.1016/j.bmcl.2018.11.058.

(10) Publicover, E. A.; Kolwich, J.; Stack, D. L.; Doué, A. J.; Ylijoki, K. E. O. Crystal Structure of (S)-Sec-Butylammonium l-Tartrate Monohydrate. *Acta Crystallogr. Sect. E Crystallogr. Commun.* **2017**, *73*, 716–719. https://doi.org/10.1107/S2056989017005448.

(11) Ghosh, T.; Ernst, M.; Hashmi, A. S. K.; Schaub, T. Ruthenium Catalyzed Direct Asymmetric Reductive Amination of Simple Aliphatic Ketones Using Ammonium Iodide and Hydrogen. *Eur. J. Org. Chem.* **2020**, *2020* (30), 4796–4800. https://doi.org/10.1002/ejoc.202000750.

(12) Goswami, A.; Guo, Z.; Parker, W. L.; Patel, R. N. Enzymatic Resolution of Sec-Butylamine. *Tetrahedron: Asymmetry* **2005**, *16* (9), 1715–1719. https://doi.org/10.1016/j.tetasy.2005.03.012.

(13) Poulhès, F.; Vanthuyne, N.; Bertrand, M. P.; Gastaldi, S.; Gil, G. Chemoenzymatic Dynamic Kinetic Resolution of Primary Amines Catalyzed by CAL-B at 38-40°c. *J. Org. Chem.* **2011**, *76* (17), 7281–7286. https://doi.org/10.1021/jo201256w.

(14) Hanson, R. L.; Davis, B. L.; Chen, Y.; Goldberg, S. L.; Parker, W. L.; Tully, T. P.; Montana, M. A.; Patel, R. N. Preparation of (R)-Amines from Racemic Amines with an (S)-Amine Transaminase from Bacillus Megaterium. *Adv. Synth. Catal.* **2008**, *350* (9), 1367–1375. https://doi.org/10.1002/adsc.200800084.

(15) Malik, M. S.; Park, E.-S.; Shin, J.-S. ω-Transaminase-Catalyzed Kinetic Resolution of Chiral Amines Using l-Threonine as an Amino Acceptor Precursor. *Green Chem.* **2012**, *14* (8), 2137. https://doi.org/10.1039/c2gc35615e.

(16) Yoon, S.; Patil, M. D.; Sarak, S.; Jeon, H.; Kim, G. H.; Khobragade, T. P.; Sung, S.; Yun, H. Deracemization of Racemic Amines to Enantiopure (R)- and (S)-Amines by Biocatalytic Cascade Employing ω-Transaminase and Amine Dehydrogenase. *ChemCatChem* **2019**, *11* (7), 1898–1902. https://doi.org/10.1002/cctc.201900080.

(17) Yun, H.; Cho, B. K.; Kim, B. G. Kinetic Resolution of (R,S)-Sec-Butylamine Using Omega-Transaminase from Vibrio Fluvialis JS17 under Reduced Pressure. *Biotechnol. Bioeng.* **2004**, *87* (6), 772–778. https://doi.org/10.1002/bit.20186.

(18) Koszelewski, D.; Clay, D.; Rozzell, D.; Kroutil, W. Deracemisation of α-Chiral Primary Amines by a One-Pot, Two-Step Cascade Reaction Catalysed by ω-Transaminases. *Eur. J. Org. Chem.* **2009**, No. 14, 2289–2292. https://doi.org/10.1002/ejoc.200801265.

(19) Mutti, F. G.; Fuchs, C. S.; Pressnitz, D.; Sattler, J. H.; Kroutil, W. Stereoselectivity of Four (R)-Selective Transaminases for the Asymmetric Amination of Ketones. *Adv. Synth. Catal.* **2011**, *353* (17), 3227–3233. https://doi.org/10.1002/adsc.201100558.

(20) Mutti, F. G.; Fuchs, C. S.; Pressnitz, D.; Turrini, N. G.; Sattler, J. H.; Lerchner, A.; Skerra, A.; Kroutil, W. Amination of Ketones by Employing Two New (S)-Selective ω-Transaminases and the His-Tagged ω-TA from Vibrio Fluvialis. *Eur. J. Org. Chem.* **2012**, No. 5, 1003–1007. https://doi.org/10.1002/ejoc.201101476.

(21) Koszelewski, D.; Lavandera, I.; Clay, D.; Rozzell, D.; Kroutil, W. Asymmetric Synthesis of Optically Pure

Pharmacologically Relevant Amines Employing ω-Transaminases. *Adv. Synth. Catal.* **2008**, *350* (17), 2761–2766. https://doi.org/10.1002/adsc.200800496.

(22) Planchestainer, M.; Contente, M. L.; Cassidy, J.; Molinari, F.; Tamborini, L.; Paradisi, F. Continuous Flow Biocatalysis: Production and in-Line Purification of Amines by Immobilised Transaminase from Halomonas Elongata. *Green Chem.* **2017**, *19* (2), 372–375. https://doi.org/10.1039/C6GC01780K.

(23) *Immobilization of Enzymes and Cells*; Guisan, J. M., Ed.; Humana Press Inc., 2013; Vol. 1051.

(24) Padrosa, D. R.; Vitis, V. De; Contente, M. L.; Molinari, F.; Paradisi, F. Overcoming Water Insolubility in Flow: Enantioselective Hydrolysis of Naproxen Ester. *Catalysts* **2019**, *9* (3), 232. https://doi.org/10.3390/catal9030232.

(25) Jaźwiński, J. Studies on Adducts of Rhodium(II) Tetraacetate and Rhodium(II) Tetratrifluoroacetate with Some Amines in CDCl3 Solution Using 1H, 13C and 15N NMR. *J. Mol. Struct.* **2005**, *750* (1–3), 7–17. https://doi.org/10.1016/j.molstruc.2005.03.035.

(26) Cerioli, L.; Planchestainer, M.; Cassidy, J.; Tessaro, D.; Paradisi, F. Characterization of a Novel Amine Transaminase from Halomonas Elongata. *J. Mol. Catal. B: Enzym.* **2015**, *120*, 141–150. https://doi.org/10.1016/j.molcatb.2015.07.009.

(27) Kaulmann, U.; Smithies, K.; Smith, M. E. B.; Hailes, H. C.; Ward, J. M. Substrate Spectrum of ??-Transaminase from Chromobacterium Violaceum DSM30191 and Its Potential for Biocatalysis. *Enzyme Microb. Technol.* **2007**, *41* (5), 628–637. https://doi.org/10.1016/j.enzmictec.2007.05.011.

(28) Heckmann, C. M.; Gourlay, L. J.; Dominguez, B.; Paradisi, F. An (R)-Selective Transaminase From Thermomyces Stellatus: Stabilizing the Tetrameric Form. *Front. Bioeng. Biotechnol.* **2020**, *8*, 707. https://doi.org/10.3389/fbioe.2020.00707.

(29) Höhne, M.; Schätzle, S.; Jochens, H.; Robins, K.; Bornscheuer, U. T. Rational Assignment of Key Motifs for Function Guides in Silico Enzyme Identification. *Nat. Chem. Biol.* **2010**, *6* (11), 807–813. https://doi.org/10.1038/nchembio.447.

(30) Theodorou, D.; Zannikou, Y.; Zannikos, F. Estimation of the Standard Uncertainty of a Calibration Curve: Application to Sulfur Mass Concentration Determination in Fuels. *Accredit. Qual. Assur.* **2012**, *17* (3), 275–281. https://doi.org/10.1007/s00769-011-0852-4.

(31) *Eurachem/CITAC Guide: Quantifying Uncertainty in Analytical Measurement*, 3rd ed.; Ellison, S. L. R., Williams, A., Eds.; 2012. https://doi.org/0 948926 15 5.

(32) Dall'Oglio, F.; Contente, M. L.; Conti, P.; Molinari, F.; Monfredi, D.; Pinto, A.; Romano, D.; Ubiali, D.; Tamborini, L.; Serra, I. Flow-Based Stereoselective Reduction of Ketones Using an Immobilized Ketoreductase/Glucose Dehydrogenase Mixed Bed System. *Catal. Commun.* **2017**, *93*, 29–32. https://doi.org/10.1016/j.catcom.2017.01.025.

(33) Guidi, B.; Planchestainer, M.; Contente, M. L.; Laurenzi, T.; Eberini, I.; Gourlay, L. J.; Romano, D.; Paradisi, F.; Molinari, F. Strategic Single Point Mutation Yields a Solvent- and Salt-Stable Transaminase from Virgibacillus Sp. in Soluble Form. *Sci. Rep.* **2018**, *8* (1), 16441. https://doi.org/10.1038/s41598-018-34434-3.

(34) Pavlidis, I. V.; Weiß, M. S.; Genz, M.; Spurr, P.; Hanlon, S. P.; Wirz, B.; Iding, H.; Bornscheuer, U. T. Identification of (S)-Selective Transaminases for the Asymmetric Synthesis of Bulky Chiral Amines. *Nat. Chem.* **2016**, *8* (July), 1076–1082. https://doi.org/10.1038/NCHEM.2578.

(35) Guo, F.; Berglund, P. Transaminase Biocatalysis: Optimization and Application. *Green Chem.* **2017**, *19* (2), 333–360. https://doi.org/10.1039/C6GC02328B.

(36) Planchestainer, M.; Hegarty, E.; Heckmann, C. M.; Gourlay, L. J.; Paradisi, F. Widely Applicable Background Depletion Step Enables Transaminase Evolution through Solid-Phase Screening. *Chem. Sci.* **2019**, *10* (23),

5952–5958. https://doi.org/10.1039/c8sc05712e.

(37) Trott, O.; Olson, A. J. AutoDock Vina: Improving the Speed and Accuracy of Docking with a New Scoring Function, Efficient Optimization, and Multithreading. *J. Comput. Chem.* **2009**, *31* (2), 455–461. https://doi.org/10.1002/jcc.21334.

(38) Schätzle, S.; Höhne, M.; Redestad, E.; Robins, K.; Bornscheuer, U. T. Rapid and Sensitive Kinetic Assay for Characterization of ω-Transaminases. *Anal. Chem.* **2009**, *81* (19), 8244–8248. https://doi.org/10.1021/ac901640q.

For Table of content use only

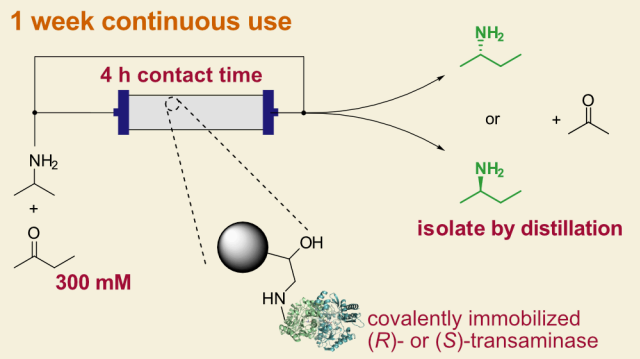

Synopsis

A transaminase catalysed synthesis of both enantiomers of 2-aminobutane is being described, generating mainly biodegradable waste, and avoiding the use of organic solvents.